Chapter 11

Corrosion Resistance and Tribological Properties of Epoxy Coatings Reinforced with Well-Dispersed Graphene

Liu Shuan

Additional information is available at the end of the chapter

http://dx.doi.org/10.5772/64097

Abstract

Seawater environment is the most harsh corrosion media, thus the deterioration of metal materials in marine environment is particularly serious. Organic coatings are good options for metal protection. Regarding the large impact of metal corrosion on marine engineering and the important significance of metal anticorrosion, this chapter deals with the research and development of the protective mechanism, wear resistance, and antifriction properties of the graphene-based epoxy coating used in marine environment. A highly efficient physical graphene dispersant was obtained by organic synthesis, and the graphene powder was dispersed uniformly in organic solvent and then added into epoxy resin. Moreover, the structure-activity relationship of the graphene-based epoxy coating was systematically investigated, taking into account its different amounts and dispersing characteristics in seawater. Consequently, the corrosion behavior and protection mechanism of the graphene-based heavy anticorrosion coating are evaluated and clarified. The obtained results are of fundamental importance for the field.

Keywords: grapheme, corrosion resistance, tribology, epoxy coating, dispersion

1. Introduction

The inhabitants of modernized nations live in metal-based societies. Almost all common metals or steels tend to react with their environments to some extents and at different corrosion rates. Corrosion is defined as the deterioration of a material, usually a metal, that requires the presence

of an anode, a cathode, an electrolyte, and an electrical circuit [1]. Corrosion usually occurs as a natural phenomenon.

The sea occupies about three-quarters of the Earth and has several kinds of chemical ions. Seawater is a powerful natural corrosion environmental, which contains almost all of the elements present on the Earth. Some of these chemicals or ions (e.g., Cl^-, SO_4^{2-}) are corrosive towards metals. Corrosion damages considerably the marine steel infrastructures, such as ships, offshore oil installations, submarine pipelines, and port terminals, which not only causes serious economic losses but also threats the safety of human life and ecology [2, 3]. It has been estimated that the metal corrosion losses in China totaled one trillion and eight hundred billion in 2014, which accounted for one-third of the average gross national product (GNP). Marine corrosion accounts for the majority of metal losses. Thus, an effective protection technology is necessary to inhibit corrosion. Up to now, several methods have been used to protect metals against corrosion such as cathodic protection, protective coating, corrosion inhibitors, and addition of alloy elements. Among those procedures, coating is the most effective and economical way to inhibit metal corrosion, as it can block the contact of the corrosive medium with the metal [4].

1.1. Anticorrosion and failure mechanism of organic coating

Organic coatings can be found everywhere in industrialized nations, in order to protect metal structures and metal equipment. They can protect metals from corrosion in two ways. First, the coating film acts as a physical barrier to separate the metal substrate from the corrosive environment. Second, the organic coating can contain corrosion inhibitors, which decrease the corrosion rate of the metal.

However, organic coatings are not perfect barriers as they can be penetrated by corrosive media, such as oxygen, water molecule, and ions. When this happens, metal corrosion can occur underneath the organic coating/metal interface. Thus, the corrosive media accumulated beneath the organic coating not only leads to metal corrosion but also decreases the adhesion of the coating to the metal. Moreover, the corrosion products formed on the metal surface can also destroy the coating/metal system. Generally, there are three methods often used to improve the protective performance of the organic coatings. First, fillers or pigments, such as graphene, nanoclay, ZnO, and MoS_2, are added into the coating to extend the diffusion path of corrosive media through the coating. Second, corrosion inhibitors are added to inhibit metal corrosion reaction underneath the coating. Third, high density, high cross-linked, thicker, and self-healing coating are needed to reduce the coating permeability [5].

1.2. Graphene based epoxy coating used for metal protection

Graphene (G) is a two-dimensional material with a single layer of around 0.335 nm and a diameter ranging from a few to several hundred microns. It has attracted increasing attention from academic and industrial fields due to their unique nanostructure, excellent physical properties, large specific surface area, super hydrophobic properties, and good compatibility with polymer matrixes [6, 7]. It has been reported that G can exhibit extraordi-

http://dx.doi.org/10.5772/64097

nary corrosion resistance and self-lubricant characteristics due to its unique flexible graphitic layers, super-hydrophobic characteristics, extremely high strength, and easy shear capability on its densely packed and atomically smooth surface [8]. However, G nanosheets are prone to aggregate due to their strong van der Waals forces and high specific surface areas, which is difficult in achieving an homogenous dispersion of G in organic coatings. Many works on chemical modification approach have been reported to improve dispersion of G in composite coatings [9–11]. For example, Chang et al. [12] reported on the preparation of polyimide grafted G via a thermal imidization reaction. The well-dispersed G/polyimide coatings provided advanced corrosion protection of cold-rolled steel, as compared to neat polyimide coating. Compared to chemical modification, simply dispersing G into a polymer matrix can be particularly advantageous due to less damage made to G, and the high efficiency and ease of the preparation method.

In this chapter, the fabrication of composite coatings (with epoxy coating as the organic matrix and uniform dispersed G as anticorrosive barrier) is reported. The corrosion resistance and tribological properties of epoxy coatings reinforced with well-dispersed G are evaluated in details.

2. Corrosion resistance and tribological properties of G/epoxy composite coating

2.1. G powder dispersion performance in organic solvent

G was supplied by Ningbo Morsh Technology Company from China. Four different physical G dispersants, namely dispersant-1 (it has a basic triphenylmethane structure), dispersant-2 (it is a sodium polyacrylate), dispersant-3 (it is a sodium hexametaphosphate), dispersant-4 (it has a carboxylated oligoaniline structure), were synthesized and used to disperse G. **Figure 1** depicts the G powder dispersed in ethanol solution by the different G dispersants after 30 days. Without any dispersant, the G powder was aggregated and quickly precipitated at the bottom of the container (**Figure 1a**). Dispersants-1 can be adsorbed on the surface of G, however, the Dispersants-1/G system precipitated after a few hours (**Figure 1b**); for Dispersants-2 and Dispersants-3, G powder was swelled and can be dispersed, but G precipitated after 12 h (**Figure 1c** and **d**). Dispersant-4 was able to stably disperse G in ethanol after even 30 days (**Figure 1e**), only a few G slurry can be found at bottom of glass bottle. Interestingly, when the dispersed G was dried by spraying, it still could be re-dispersed in several solvents, such as water, tetrahydrofuran (THF), and ethanol (**Figure 2**). **Figure 3** shows the SEM images of dispersed G in ethanol solution. It can be seen that the layered G was completely dispersed at length of ~5 μm, and no obvious aggregates existed. **Figure 4** depicts an atomic force microscopy (AFM) image of dispersed G deposited on a Si-coated substrate. On the topography image (**Figure 4a**), the G layer can be seen as slightly brighter than the Si-coated substrate. From the line scan shown in **Figure 4b**, it is very easy to estimate the thickness of G layer (about 3–6 nm), indicating that the aggregated G was exfoliated to ultra-thin layers.

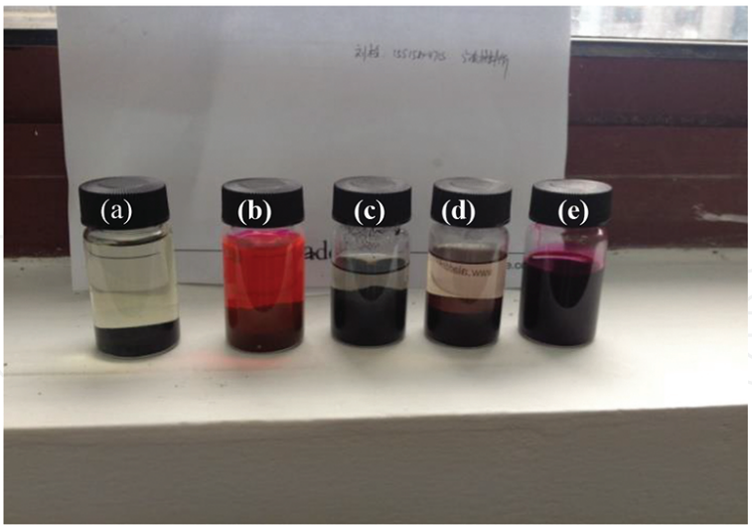

Figure 1. G powder dispersed in ethanol solution using different G dispersants after 30 days; the mass ratio of dispersant to G powder was 1:5. (a) G+ethanol; (b) G+dispersant-1+ethanol; (c) G+dispersant-2+ethanol; (d) G+dispersant-3+ethanol; (e) G+dispersant-4+ethanol.

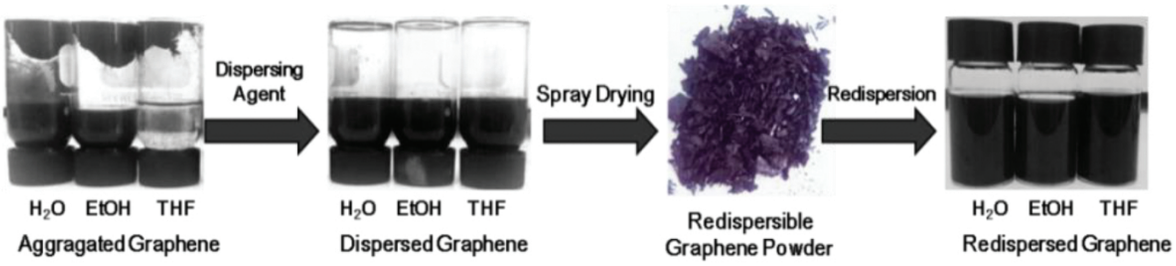

Figure 2. Schematic diagram of G dispersion and re-dispersion in different solvents.

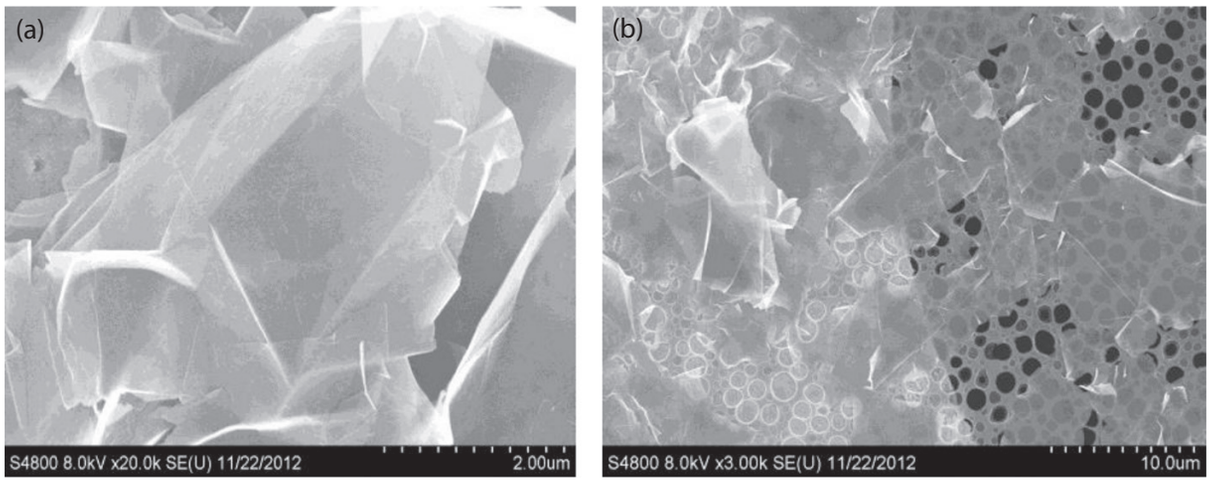

Figure 3. SEM images of dispersed G at low magnification (a) and high magnification (b).

http://dx.doi.org/10.5772/64097

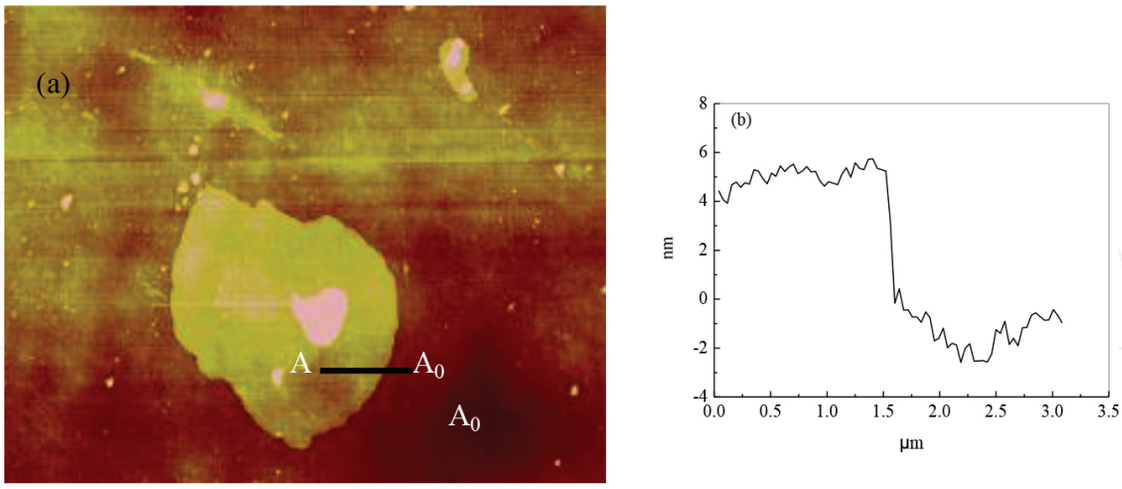

Figure 4. AFM images (a) of a thin G film deposited on a Si-coated substrate and height profile (b) along the black line (from A to A_0).

2.2. Preparation of a G/epoxy composite coating

Figure 5 depicts the preparation process of G-based epoxy coatings. The well-dispersed G was mixed in the epoxy resin and cured by a polyamide agent (650 polyamide curing agent, light yellow, Amine value: 420 mgKOH/g, viscosity: 18,000 mPa s/40°C). **Figure 6a** and **b** shows typical SEM micrographs of fracture surfaces (cross section) of an epoxy coating containing 0.5 wt% G. It is well known that the fracture surface of pure epoxy thermoset exhibits oriented "bamboo"-like fracture patterns starting from the cracks. In contrast, this G based epoxy coating showed less brittle-like fracture morphology. The existence of highly dispersed G effectively disturbs the crack propagation due to its two dimensional nanostructure. **Figure 7** depicts TEM images of G (0.5 wt%) in epoxy coatings. It is shown that G is randomly dispersed in the coatings, and the good dispersion of G can extend the diffusion path of corrosive media in the epoxy coating.

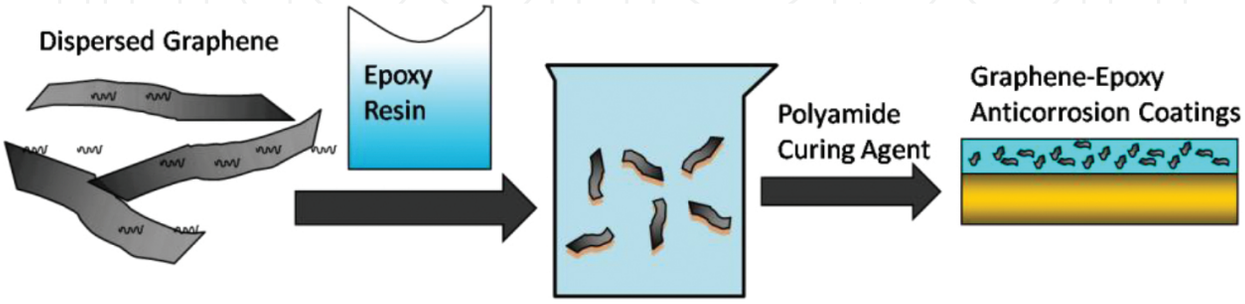

Figure 5. Preparation process of G/epoxy composite coatings.

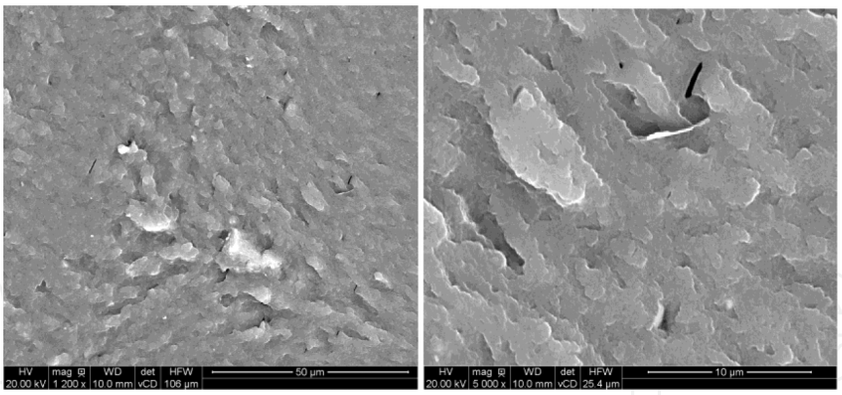

Figure 6. SEM images of cross sections of a G/epoxy composite coating (0.5 wt% G content).

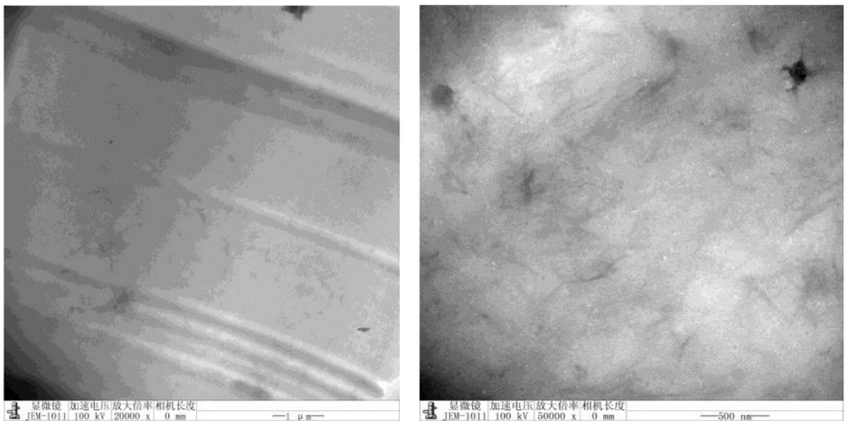

Figure 7. TEM images of a G/epoxy composite coating (0.5 wt% G content).

2.3. Corrosion resistance and mechanism of G/epoxy composite coating

In order to evaluate the improvement obtained with the G/epoxy composite coating, the pure epoxy coating, the D4/epoxy coating, and the G/epoxy coating were prepared in a similar way to the described above for the G-D4/epoxy coating (D4 means dispersant 4, it has a carboxylated oligoaniline structure). Electrochemical measurements were performed on a CHI-660E electrochemical workstation in 3.5% NaCl solution at room temperature. A three-electrode set-up was used for EIS test, a saturated calomel electrode (SCE) was used as the reference electrode, a platinum plate of 2.5 cm^2 as the counter electrode, and coating/Q235 steels as the working electrode. Before electrochemical impedance spectroscopy (EIS) measurement, the coating/Q235 steel specimen was initially kept at an open circuit potential (OCP) for 1 h until a stable state was attained. For EIS, the test frequency range was 10^5 to 10^{-2} Hz and the amplitude of the sinusoidal voltage signal was 20 mV. ZsimpWin 3.21 software was used to fit the EIS spectra.

Figure 8 shows the open circuit potential (E_{OCP}) variation of pure epoxy, G/epoxy, D4/epoxy, and G-D4/epoxy as a function of immersion time in 3.5% NaCl solution. The E_{OCP} of all coatings

http://dx.doi.org/10.5772/64097

decreased to different degrees after the fluctuation at initial time and then remained basically unchanged after 16 days. Compared with pure epoxy, D4/epoxy and G-D4/epoxy exhibit a larger E_{OCP}, whereas G/epoxy displays a E_{OCP} similar to that of the pure epoxy. The positive shift of E_{OCP} for 0.30 V for G-D4/epoxy and 0.10 V for D4/epoxy after 35-day immersion shows that the G-D4 hybrid and D4 have obvious corrosion inhibition properties, and a similar phenomenon was reported by other researchers [13]. Furthermore, the G-D4 hybrid exhibits better corrosion inhibition than D4, while commercial G without D4 functionalization has almost no corrosion inhibition.

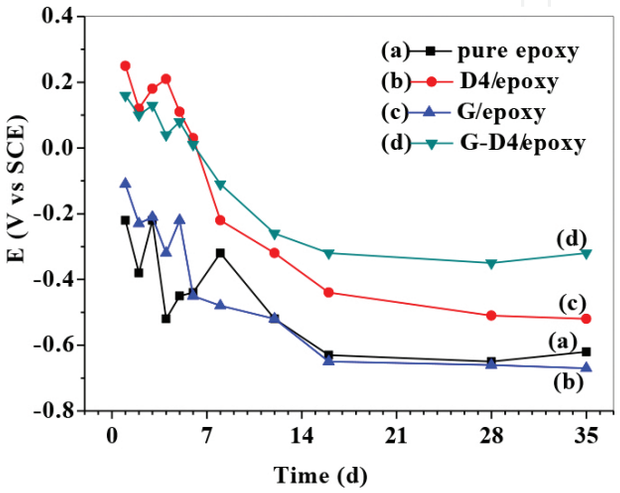

Figure 8. Time dependence of the open circuit potential (E_{OCP}) of pure epoxy (a), G/epoxy (b), D4/epoxy (c) and G-D4/epoxy (d) coated Q235 steel electrodes immersed in 3.5% NaCl solution.

EIS was further employed to investigate the corrosion mechanism and evaluate the degradation processes of the G-D4/epoxy composites, as shown in **Figure 9**. The Bode phase plots show one time constant at the initial stage of immersion (stage I), and then two time constants appeared due to the penetration of corrosive media during the immersion process (stage II). Usually, the time constant at the high frequency range can be attributed to the coating layer, while the one time constant at lower frequencies corresponds to a corrosion process taking place at the metal/coating interface. The pure epoxy, G/epoxy, and D4/epoxy coatings exhibit two time constants in short term immersion (2 days, 1 day, and 4 days, respectively), while the G-D4/epoxy coating shows one time constant in a high frequency range for 28-day immersion. The impedance modulus at low frequency ($|Z|_{0.01Hz}$) can represent the corrosion protection of coating/metal system, which is in inverse proportion to corrosion rate. The $|Z|_{0.01Hz}$ of the G-D4/epoxy-coated Q235 electrode was 1.6×10^9 Ω cm^2 after 16-day immersion (**Figure 9D**), which was far larger than that of pure epoxy (2.2×10^7 Ω cm^2), G/epoxy (3.1×10^6 Ω cm^2), and D4/epoxy (5.5×10^7 Ω cm^2)-coated electrodes after 12-day immersion (**Figure 9A–C**). These results indicate that the G-D4/epoxy coating provides better corrosion protection for the Q235 steel than other coatings. The increase in impedance for G-D4/epoxy coating can be attributed to the hydrophobicity and barrier effects of the well dispersed graphene.

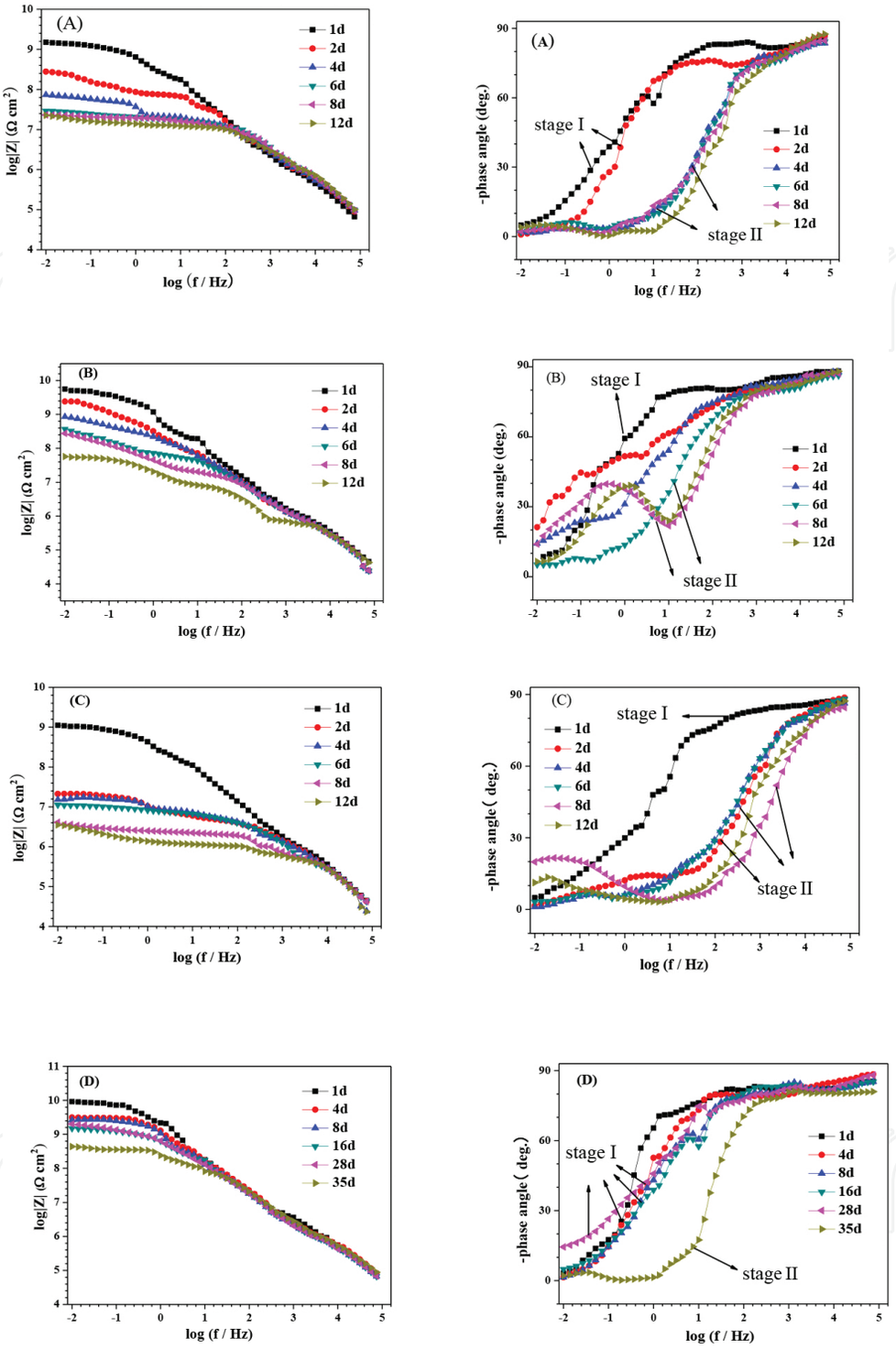

Figure 9. Bode plots of pure epoxy (A), D4/epoxy (B), G/epoxy (C), and G-D4/epoxy (D) coated Q235 steel electrodes immersed in 3.5% NaCl solution after different times.

Water uptake of the coating was calculated based on the changes of the coating capacitance due to the variation of the dielectric constant. The water diffusion coefficient D could be calculated by means of the simplified Fick's second law of diffusion [14] (see Eq. (**1**)):

http://dx.doi.org/10.5772/64097

$$\frac{\lg Q_c - \lg Q_0}{\lg Q_\infty - \lg Q_0} = \frac{2}{L}\sqrt{\frac{D}{\pi}}\sqrt{t} \tag{1}$$

where Q_0, Q_c, and Q_∞ are the coating capacitances at the beginning of the immersion time t_0, the time t_c, and the time in saturated water absorption state t_∞, respectively. D is the diffusion coefficient, L is the coating thickness. The coating capacitances obtained from the fitted corrosion parameters, were fitted with equivalent circuits (**Figure 10**) by ZsimpWin 3.21 software. D can be calculated from the $\lg Q_c - t^{1/2}$ curves (**Figure 11**), yielding the water diffusion coefficients of these 4 coating (pure epoxy, G/epoxy, D4/epoxy, and G-D4/epoxy), calculated to be 2.25×10^{-12}, 23.6×10^{-12}, 17.1×10^{-12} s and 0.619×10^{-12} cm^2/s, respectively (**Figure 12**). The significant decrease of water diffusion coefficient for G-D4/epoxy coating confirmed that the water penetration into the epoxy coating was impeded by the highly dispersed G, while the G/epoxy coatings without D4 exhibited much higher water diffusion coefficient due to the aggregation of G.

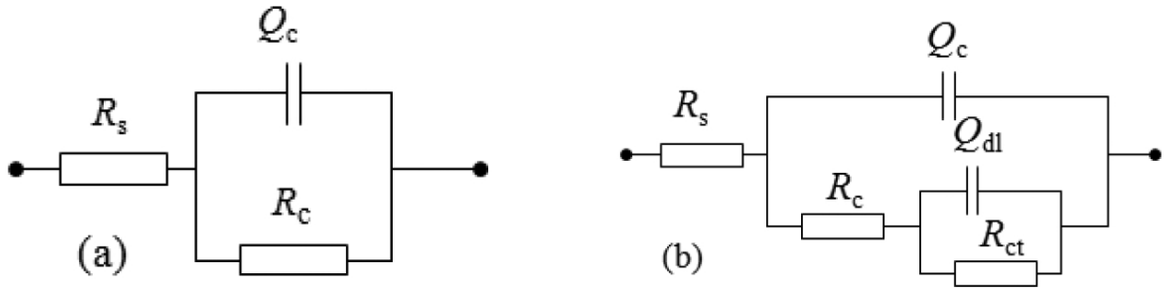

Figure 10. The equivalent circuit (a) for stage I and (b) for stage II used to fit the EIS data.

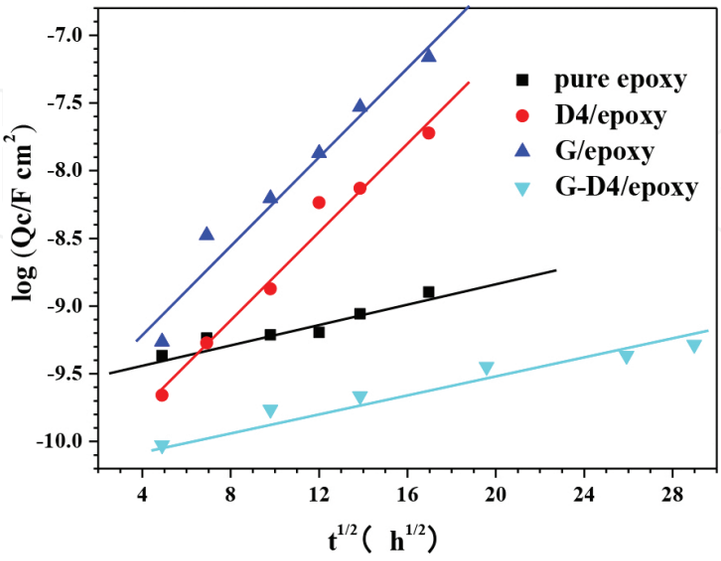

Figure 11. $\lg Q_c - t^{1/2}$ curves of different composite coatings immersed in 3.5% NaCl solution.

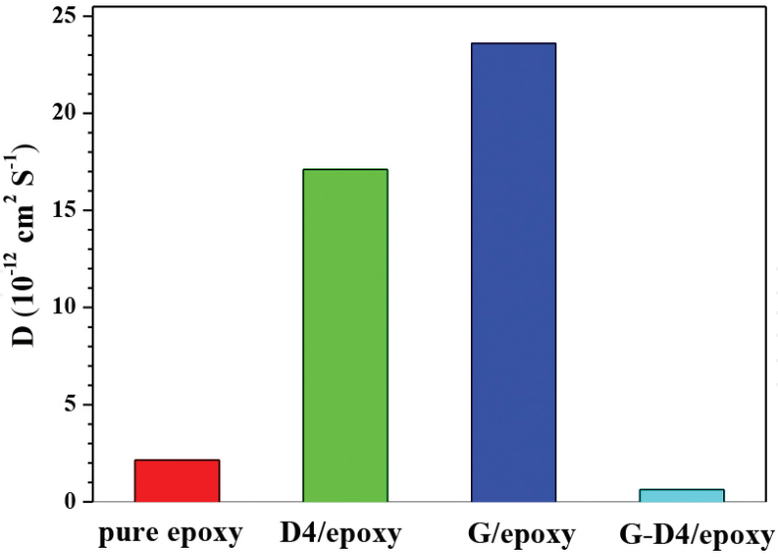

Figure 12. The water diffusion coefficient D of different composite coatings immersed in 3.5% NaCl solution.

2.4. Tribological properties of graphene/epoxy composite coating

The coefficient of friction (COF) was conducted on UMT-3 tribometer (UMT-3, Bruker-CETR, USA) with a ball-on-plate configuration using the following conditions: load of 3N, sliding velocity of 1 Hz, friction duration of 20 min, and wear track length of 5 mm. All the experiments were performed under dry condition and seawater lubricated condition. **Figure 13** shows the friction coefficient of the G/epoxy coatings as function of test time under both of dry sliding and seawater lubrication, respectively. It was clear that the COF of G/epoxy coatings initially increases rapidly and then reaches stability with time in dry conditions, but in seawater environment, the COF of G/epoxy coatings initially decrease and then reach a stable state. The COF values of neat epoxy coating, 0.25%G-epoxy coating, and 0.5%G-epoxy coating were 0.49,

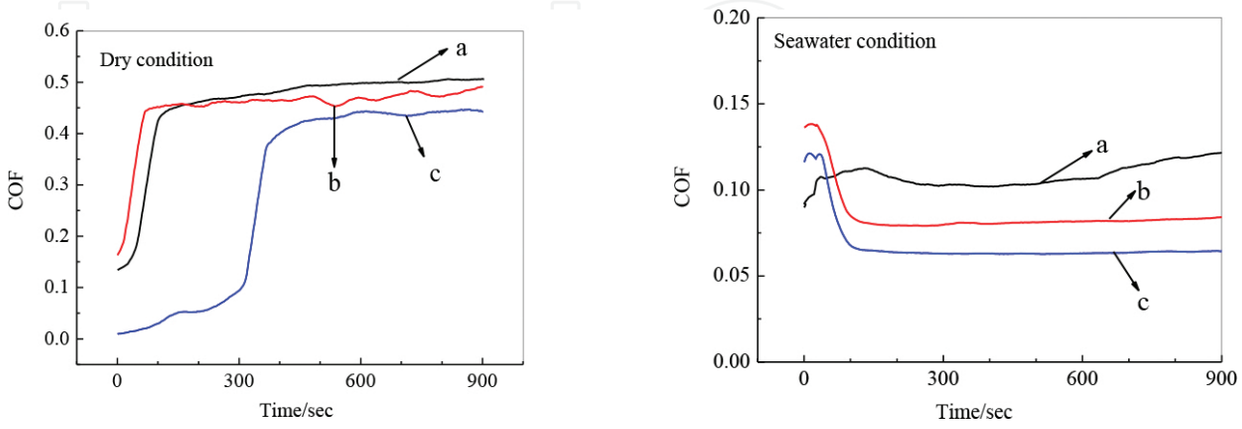

Figure 13. COF of three G-epoxy coating in dry and seawater friction conditions. (a) Neat epoxy coating; (b) 0.25%G-epoxy coating; (c) 0.5%G-epoxy coating.

0.45, and 0.42 in dry conditions, respectively. The COF values of neat epoxy coating, 0.25%G-epoxy coating, and 0.5%G-epoxy coating were 0.12, 0.08, and 0.06 in seawater, respectively. These results suggest that G can decrease the COF values of epoxy coatings in both dry and seawater conditions.

The wear traces of the different coatings were evaluated by using a surface profiler (Alpha-Step IQ, KLA-Tencor, USA). The wear resistance of the coatings is represented by wear trace cross-sectional area on account of the uniform wear trace length. **Figure 14** shows the wear trace areas of G/epoxy coatings with different mass ratio of G measured under dry sliding and seawater lubrication. It can be seen that the wear trace areas of composite coatings decreased with the increase of G content in G/epoxy coatings. In addition, the COF and wear traces area, under seawater lubrication, were much lower than those under dry sliding, during the whole process. Three main factors can cause these phenomena: First, the lubricating effect of seawater can effectively reduce the direct contact of the composite coatings with the counterpart surface. Second, the seawater medium can act as coolant which significantly reduces the friction heat, avoiding thermal softening, and resulting in lower COF and wear traces area. Finally, the wear debris can be continuously removed by seawater, leading to smooth and clean worn surface.

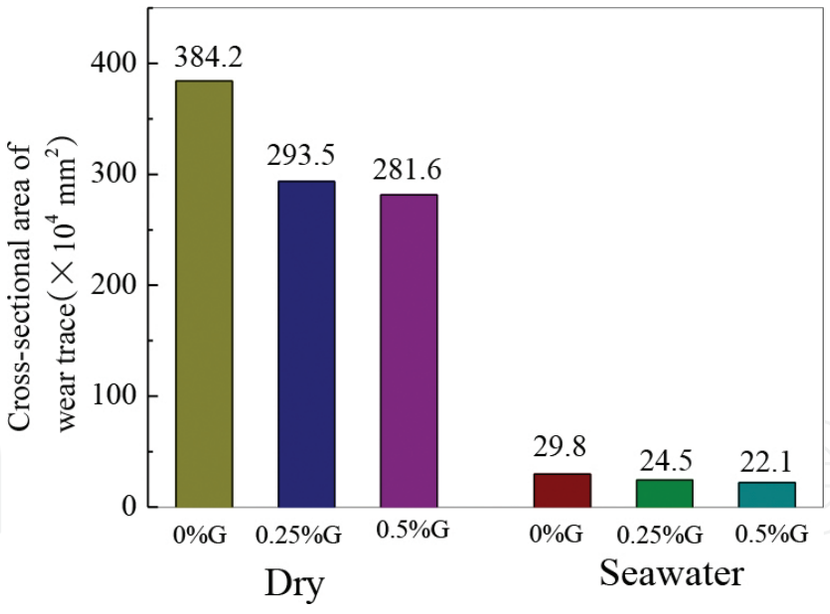

Figure 14. Cross-sectional area of wear trace of three G-epoxy coatings in dry and seawater friction conditions.

3. Conclusions

1. Graphene (G) can be uniformly dispersed in several solvents.

2. The well-dispersed G can block the coating pores and decrease the electrolyte diffusion towards the epoxy coating, the water diffusion coefficients of epoxy coating decrease with addition of 0.5 wt% G.

3. G increases the corrosion resistance of epoxy coatings.

4. Friction coefficient and wear rate of the epoxy coating decrease with the addition of G; the friction coefficient and wear rate of G/epoxy composite coating in seawater was lower than in dry conditions.

Acknowledgments

The authors wish to acknowledge the financial support of the National Science Foundation of China (No. 41506098), China Postdoctoral Science Foundation (No. 2015M580528), Zhejiang Province Preferential Postdoctoral Science Foundation (No. BSW1502160) and Open Fund Project of Key Laboratory of Marine Materials and Related Technologies (LMMT-KFKT-2014-008) in Chinese Academy of Sciences.

Author details

Liu Shuan

Address all correspondence to: liushuan@nimte.ac.cn

Ningbo Institute of Materials Technologies and Engineering, Chinese Academy of Sciences, Ningbo, China

References

[1] E McCafferty. Introduction to Corrosion Science. Springer, Alexandria Va, USA ,2009.

[2] S Liu, H Y Sun, N Zhang, et al. The corrosion performance of galvanized steel in closed rusty seawater. International Journal of Corrosion, 2013 (2013) 1–9.

[3] S Liu, H Y Sun, L J Sun, et al. Effects of pH and Cl^- concentration on corrosion behavior of the galvanized steel in simulated rust layer solution. Corrosion Science, 65 (2012) 520–527

[4] L Gu, S Liu, H C Zhao, et al. Anticorrosive oligoaniline-containing electroactive siliceous hybrid materials. RSC Advance, 5 (2015) 56011–56019.

[5] B Chen, J Ma, L Gu, et al. Anticorrosive properties of oligoaniline containing photo-cured coatings. International Journal of Electrochemical Science, 10 (2015) 9154–9166.

[6] L Gu, S Liu, H C Zhao, et al. Facile Preparation of water-dispersible graphene sheets stabilized by carboxylated oligoanilines and their anticorrosion coatings. ACS Applied Materials and Interfaces, 7 (2015) 17641–17648.

[7] S Liu, L Gu, H C Zhao, et al. Corrosion resistance of graphene-reinforced waterborne epoxy coatings. Journal of Materials Science & Technology, 2013, 32(5) : 425–431.

[8] C M Kumar, T V Venkatesha, R. Shabadi. Preparation and corrosion behavior of Ni and Ni–graphene composite coatings. Materials Research Bulletin, 48 (2013) 1477–1483.

[9] B Ramezanzadeh, E Ghasemi, M Mahdavian, E Changizi, M H Mohamadzadeh. Covalently-grafted graphene oxide nanosheets to improve barrier and corrosion protection properties of polyurethane coatings. Carbon, 93 (2015) 555–573.

[10] C H Chang, T C Huang, C W Peng, et al. Novel anticorrosion coatings prepared from polyaniline/graphene composites. Carbon, 50 (2015) 5044–5051.

[11] Q F Jing,W S Liu, Y Z Pan, et al. Chemical functionalization of graphene oxide for improving mechanical and thermal properties of polyurethane composites. Materials and Design 85 (2015) 808–814.

[12] K C Chang, C H Hsu, H I Lu, et al. Advanced anticorrosive coatings prepared from electroactive polyimide/graphene nanocomposites with synergistic effects of redox catalytic capability and gas barrier properties. Express Polymer Letters, 8 (2014) 243–255.

[13] H Wei, D Ding, S Wei, et al. Anticorrosive conductive polyurethane multiwalled carbon nanotube nanocomposites. Journal of Materials Chemistry A, 1 (2013) 10805–10813.

[14] M M Wind, H J W Lenderink. A capacitance study of pseudo-Fickian diffusion in glassy polymer coatings. Progress in Organic Coatings, 28 (1996) 239–250.

IntechOpen